14th IEA Heat Pump Conference
15-18 May 2023, Chicago, Illinois

A heat pump system for simultaneous comfort floor cooling and domestic hot water

Tingting Zhu[a,b*], Jierong Liang[b], Jan Eric Thorsen[c], Oddgeir Gudmundsson[c], Wilko Rohlfs[a], Brian Elmegaard[b]

[a]University of Twente, Drienerlolaan 5, Enschede 7522 NB , The Netherlands
[b]Technical University of Denmark, Anker Engelunds Vej 101, Lyngby 2800, Denmark
[c]Danfoss A/S, Nordborgvej 81, Nordborg 6430, Denmark

Abstract

The benefit of ultra-low temperature district heating systems (ULTDH) is their low supply temperature, which increases the heat generation efficiency and significantly reduces the heat loss of the DH network. The present study proposed a dual-effect heat pump system, which in combination of the ULTDH network, fulfills both, comfort floor cooling/heating and domestic hot water (DHW) demands. Depending on the operation the ULTDH system is used as a heat source, DHW preparation, or as a heat sink in cooling operation mode. The application potential of the proposed heat pump unit used for comfort floor cooling has been validated. The cooling experimental tests were performed under designed conditions with fixed heat source temperature (22 °C) and different heat sink temperatures, simulating either DHW preparation or delivering the surplus heat to the ULTDH network. The coefficient of performance (COP) of the dual-effect heat pump system varied from 2.22 to 2.81 in cooling mode, and from 3.0 to 3.4 in heating mode. The cooling capacity ranged from 2.9 kW to 3.4 kW and heating capacity ranged from 3.8 kW to 4.4 kW.

Selection and/or peer-review under the responsibility of the organizers of the 14th IEA Heat Pump Conference 2023.

Keywords: Dual-effect; Comfort cooling; Ultra-low district heating; Cooling capacity; Domestic hot water.

1. Introduction

The amount of energy used for heating and domestic hot water (DHW) is high and will keep increasing [1]. Combined cooling and heating systems can achieve efficient utilization of resources and energy through heat recovery, which is providing sustainable solutions to global warming and the energy crisis [2]. A novel compression/ejection transcritical CO_2 heat pump system for simultaneous cooling and heating can realize the utilization of geothermal energy and solar energy [3]. Heat pumps for simultaneous heating and cooling appear as interesting solutions for electric energy saving and residential buildings with a specific mode for DHW production. An air-source heat pump has been investigated by Byrne and Ghoubali [4], which shows a good potential in producing of hot water and chilled air simultaneously.

The idea of the present study is to indicate the performance and application potential of small heat pump used in household comfort floor cooling and domestic hot water supply. Thus, a comfort cooling heat pump prototype has been set up at Technical University of Denmark (DTU) to conduct the investigation experimentally. Thermal behavior of a small heat pump unit with R134a as working refrigerant has been analyzed based on experimental results. The experimental tests were performed under design conditions: different inlet temperature for the heat source, and a fixed inlet temperature for heat sink, which corresponds to the district heating temperature supply and comfort floor cooling temperature. The variations of the heat pump operation for different temperature combinations of district heat water are outlined. The operation parameters are: 3 kW cooling capacity (50 W/m^2 for 40 m^2 room area), with a water temperature inflow of 17 °C and return of 22 °C.

* Corresponding author. Tel.: +31 53 489 8823; fax: +31 53 4893471.
E-mail address: t.zhu@utwente.nl

The application potential of the proposed heat pump unit used for comfort floor cooling has been validated experimentally. Thermal behavior and exergy performance of this small heat pump unit have been analyzed. The variations in heat pump operation under different temperature combinations of DHW are outlined. The structure of this paper is summarized as follows. In Section 2, the experimental setup and the configuration of a comfort cooling heat pump system are introduced. Then, the energy and exergy analysis method to assess the performance of the proposed system has been conducted in Section 3. In Section 4, the results are discussed considering the application scenarios. Finally, the conclusions are summarized in Section 5.

2. Experimental setup and configuration description

2.1. Testing system

The heat pump experimental set up installed in DTU is designed for the application of floor comfort cooling and DHW in the DH system (Fig.1 and Fig.2). The test rig includes four sub-systems: a secondary water cycle to illustrate the DHW system and comfort floor cooling system, a refrigerant cycle with R134a as working medium, a shunt-system and a cooling system to regulate designed test temperatures. The main information of each component is listed in Table 1. The selection of each component is calculated based on heating/cooling capacity using Danfoss calculation software.

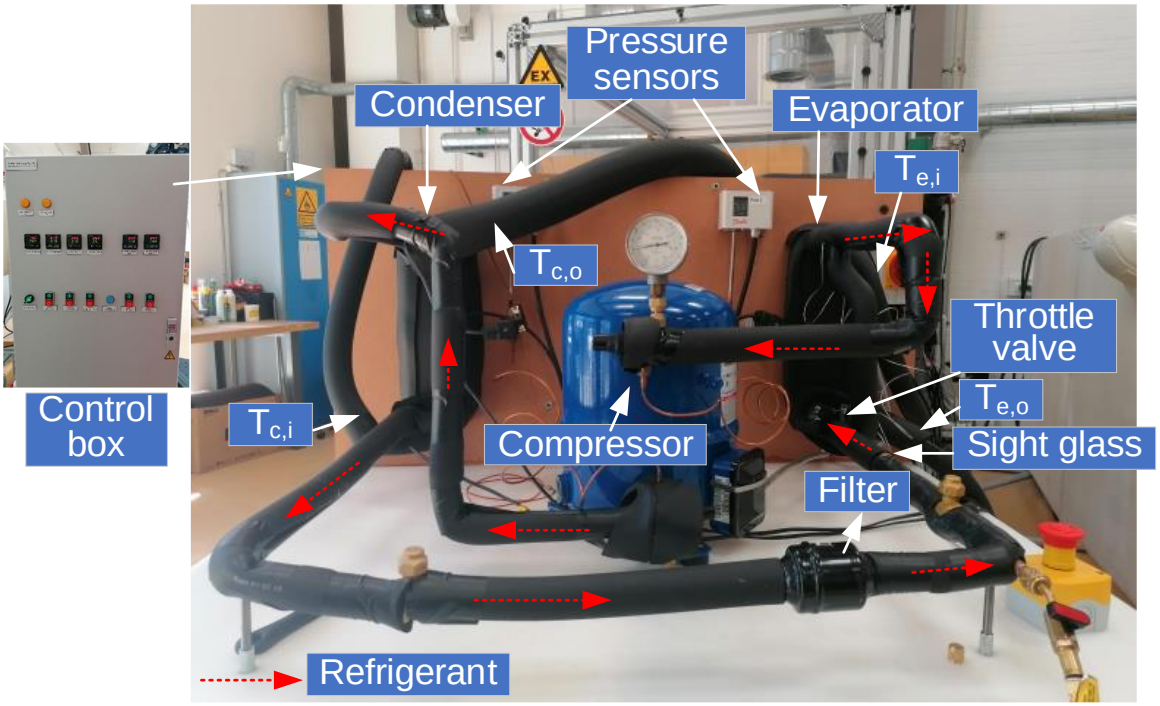

Fig. 1. Picture of Comfort Cooling test rig.

Table 1. Components information

Item	Type	Item	Type
Condenser	Danfoss D22-26	Sight Glass	Danfoss SGP 10s
Evaporator	Danfoss D22-16	TXV	Danfoss TUAE
Compressor	MTZ018-4, R134a	Orifice for TXV	Danfoss TU-6
Pressostat H	Danfoss KP7EW	Temp. sensor	Danfoss AKS-11
Pressostat L	Danfoss KP1E	Pressure sensor L	Danfoss AKS-33
Filter Dryer	Danfoss DML 053/053s	Pressure sensor H	Danfoss AKS-33

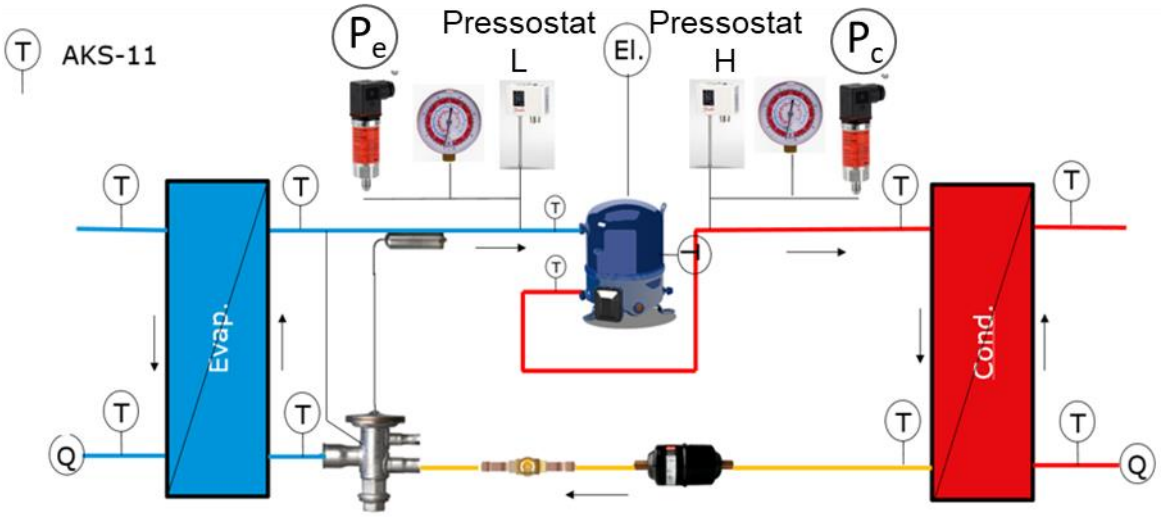

Fig. 2. Test rig diagram of comfort cooling system.

2.2. Operation conditions

A baseline heat pump system loop (1-2-3-4) used for comfort floor cooling and domestic hot water supply is sketched in Fig. 3, which consists of a compressor, a condenser, an expansion valve, and an evaporator. The dynamic process of refrigerant includes: the saturated refrigerant vapor is compressed, increasing both temperature and pressure. Subsequently, the working liquid is cooled by the water-refrigerant heat exchanger of the condenser. Afterwards, before entering the evaporator, the refrigerant turns into two-phase fluid by passing through the expansion valve. Finally, the refrigerant flows back to the compressor and the cycle is finished.

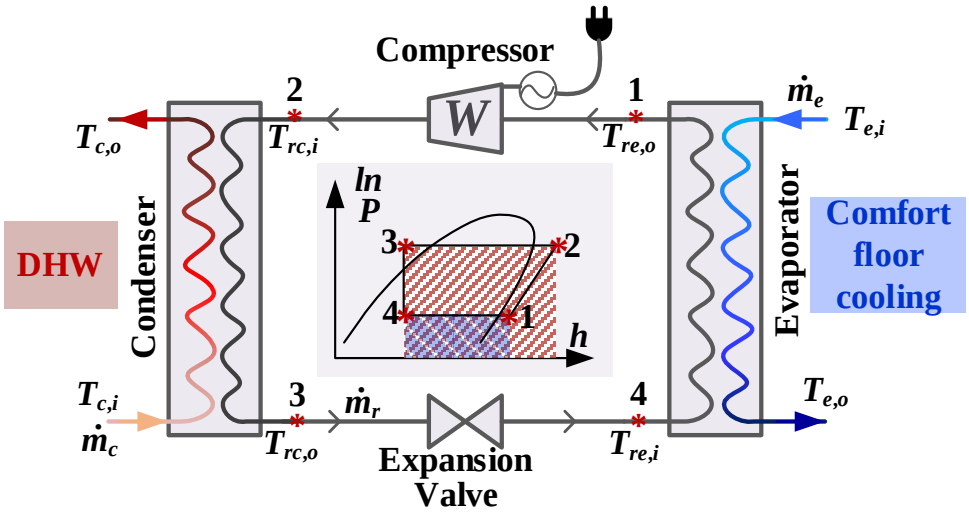

Fig. 3. Thermal-dynamic process of simultaneous comfort floor cooling and domestic hot water.

The tested parameters are listed in Table 2.

The operation conditions are chosen as below,

1) Temperature control (by electric heater and adjusting valve in the shunting system)

2) Flow control (control system to adjust valve in each of the condenser and evaporator cycle)

Parameters setting listed as,

1) Inlet water temperature of the condenser: 30 ℃, 35 ℃, 40 ℃, 45 ℃, 48.5 ℃;

2) Inlet water temperature of the evaporator: 22 ℃~27 ℃.

Experiments have been conducted on different combinations of cooling and heating temperature. Table 2 summaries the test cases.

Table 2 Tested cases

Case No.	F_c [m³/h]	F_e [m³/h]	$T_{c,i}$ [℃]	$T_{e,i}$ [℃]	Case No.	F_c [m³/h]	F_e [m³/h]	$T_{c,i}$ [℃]	$T_{e,i}$ [℃]
1	180.0	499.6	30.4	22.7	14	340.1	500.7	40.0	22.7
2	131.1	501.0	30.4	22.2	15	339.8	499.6	40.0	21.9
3	129.4	498.5	30.3	22.1	16	341.2	500.2	43.6	22.2
4	115.2	501.7	30.0	22.1	17	229.2	539.5	40.1	22.6
5	248.4	501.6	38.5	23.6	18	345.7	500.3	48.5	27.0
6	129.2	499.4	29.9	22.1	19	341.0	500.0	44.7	23.1
7	115.3	519.3	30.1	22.0	20	139.4	499.5	34.2	22.0
8	339.0	570.4	35.9	22.1	21	129.6	499.9	34.2	22.1
9	229.6	540.2	39.9	22.0	22	338.6	499.5	48.1	26.9
10	230.9	539.9	40.3	22.7	23	231.2	500.0	45.2	27.1
11	229.3	650.3	38.5	23.6	24	231.3	500.5	44.0	22.6
12	231.2	500.0	39.4	21.9	25	231.5	230.2	42.9	35.4
13	140.1	500.6	34.1	22.0					

3. Energy and exergy analysis method

3.1. Coefficient of performance (COP) of the heat pump

Due to the compressor heat loss, pipe heat loss, the temperature difference of heat transfer in evaporator and the condenser, pressure drop, and several other irreversible factors, the actual COP of the heat pump cannot reach the value of an ideal cycle. Therefore, the formula of the studied heat pump COP is,

$$\mathrm{COP}_{\mathrm{heating}} = \frac{\dot{Q}_c}{\dot{W}} \tag{1}$$

$$COP_{\mathrm{cooling}} = \frac{\dot{Q}_e}{\dot{W}} \tag{2}$$

$$\dot{Q}_c = \mathrm{c_p}\dot{m}_\mathrm{c}\,(T_{c,i} - T_{c,o}) \tag{3}$$

$$\dot{Q}_e = \mathrm{c_p}\dot{m}_\mathrm{e}\,(T_{e,i} - T_{e,o}), \tag{4}$$

where $\dot{Q}_c$ [kW] is the released heat of condenser/heat capacity; $\dot{Q}_e$ [kW] is the cooling capacity of the evaporator; W [kW] is the power of compressor; $\mathrm{c_p}$ [kJ/kg] is the specific heat capacity at constant of water; $\dot{m}_\mathrm{e}$ [kg/s] is the water mass flow rate in the evaporator; $\dot{m}_\mathrm{c}$ [kg/s] is the water mass flow rate in the condenser; $T_{c,i}$ [K]] is the inlet water temperature of the condenser; $T_{c,o}$ [K] is the outlet water temperature of the condenser; $T_{e,i}$ [K] is the inlet water temperature of the evaporator; $T_{e,o}$ [K] is the outlet water temperature of the evaporator; Figure 1 below is an example which authors may find useful.

The cooling and heating dual-effect coefficient of performance ($\mathrm{COP_{dual}}$) has been used to characterize the efficiency of the system. The measure can be defined as the sum of the absolute values of heating and cooling capacity divided by the input power,

$$\mathrm{COP_{dual}} = \frac{|\dot{Q}_{\mathrm{cooling}}|+|\dot{Q}_{\mathrm{heating}}|}{\dot{W}} \tag{5}$$

The second-law efficiency of the heat pump at the dual-effect heating and cooling working condition, $\eta_{\mathrm{II,dual}}$ can be defined as [5],

$$\eta_{\mathrm{II,dual}} = \frac{\mathrm{COP_{dual}}}{\mathrm{COP_{dual,ideal}}} \tag{6}$$

$$\mathrm{COP_{dual,ideal}} = \frac{\hat{T}_{\mathrm{c,w}}+\hat{T}_{\mathrm{e,w}}}{\hat{T}_{\mathrm{c,w}}-\hat{T}_{\mathrm{e,w}}}\ , \tag{7}$$

where $\hat{T}_{c,w}$ and $\hat{T}_{e,w}$ are average temperatures of heat supply (hot water flow through the condenser and chilled water flow through the evaporator, which are given by Eq. (8) and Eq. (9).

$$\hat{T}_{cw} = \frac{h_{\mathrm{c,o}}-h_{\mathrm{c,i}}}{s_{\mathrm{c,o}}-s_{\mathrm{c,i}}} \tag{8}$$

$$\hat{T}_{ew} = \frac{h_{\mathrm{e,i}} - h_{\mathrm{e,o}}}{s_{\mathrm{e,i}} - s_{\mathrm{e,o}}} \tag{9}$$

3.2. Exergy analysis

Compared to conventional energy analysis, the exergy analysis can accurately pinpoint the location of inefficiencies and quantitatively characterize the thermodynamic imperfection of heat transfer process and the possibility for thermodynamic development for heat pump system [6]. Thus, based on the typical thermodynamic cycle of the studied dual-effect HP (Fig. 3 pressure–enthalpy diagram) an exergy evaluation has been carried out corresponding to the exergy flow of each component. The measured quantities of the refrigerant cycle in the present study are temperatures on condenser side and pressures on both sides. The enthalpy value of the refrigerant at each state point (point Nr. 1, 2, 3 and 4, see Fig.3) can be calculated by REFPROP 10.0 software [7] with the pressure and temperature data recorded in the testing process.

The exergy balance equations of the heat pump components were described in agreement with the work of Rijs and Mróz [8] by

$$\dot{E}_{\mathrm{in}} - \dot{E}_{\mathrm{out}} = \Delta\dot{E}_{\mathrm{component}} \ , \tag{10}$$

where, $\dot{E}_{\mathrm{in}}$ [kW] is flux of exergy entering the studied thermodynamically open system; $\dot{E}_{\mathrm{out}}$ [kW] is flux of exergy leaving the studied thermodynamically open system; $\Delta\dot{E}_{\mathrm{component}}$ [kW] is the exergy loss and destruction occurring in the component.

The exergy balance equations of each component can be calculated as,

$$\Delta\dot{E}_{\mathrm{comp}} = \dot{m}_{\mathrm{r}}(h_1 - h_2 - T_0(s_1 - s_2)) + \dot{W} \tag{11}$$

$$\Delta\dot{E}_{\mathrm{cond}} = \dot{m}_{\mathrm{r}}(h_2 - h_3 - T_0(s_2 - s_3)) + \dot{m}_c \mathrm{c_p}(T_{\mathrm{c,i}} - T_{\mathrm{c,o}} - T_0 ln\frac{T_{\mathrm{c,i}}}{T_{\mathrm{c,o}}}) \tag{12}$$

$$\Delta\dot{E}_{\mathrm{TXV}} = \dot{m}_{\mathrm{r}}(h_3 - h_4 - T_0(s_3 - s_4)) \tag{13}$$

$$\Delta\dot{E}_{evap} = \dot{m}_{\mathrm{r}}\big(h_4 - h_1 - T_0(s_4 - s_1)\big) + \dot{m}_{\mathrm{e}}\mathrm{c_p}(T_{\mathrm{e,i}} - T_{\mathrm{e,o}} - T_0 ln\frac{T_{\mathrm{e,i}}}{T_{\mathrm{e,o}}}) \tag{14}$$

where, T_0 [K] is dead state temperature, (K); $\dot{m}_r$ [kg/s] is refrigerant mass flow rate of the heat pump cycle, (kg/s);

The exergy efficiency of the heat pump system writes,

$$\eta_{\mathrm{ex}} = \frac{\dot{E}_{\mathrm{use}}}{\dot{W} + \Delta\dot{E}_{\mathrm{HS}}} \ , \tag{15}$$

where

$$\dot{E}_{\mathrm{use}} = \dot{m}_{\mathrm{c}} c_{\mathrm{w}}(T_{\mathrm{c,o}} - T_{\mathrm{c,i}} - T_0 \ln\frac{T_{\mathrm{c,o}}}{T_{\mathrm{c,i}}}) \tag{16}$$

$$\Delta\dot{E}_{HS} = \dot{m}_{\mathrm{e}} c_{\mathrm{w}}(T_{\mathrm{e,i}} - T_{\mathrm{e,o}} - T_0 \ln\frac{T_{\mathrm{e,i}}}{T_{\mathrm{e,o}}}) \ , \tag{17}$$

where η_{ex} exergy efficiency of the heat pump system; $\dot{E}_{\mathrm{use}}$ [kW] is useable exergy, which is the physical exergy of the heated water via condenser; $\Delta\dot{E}_{\mathrm{HS}}$ [kW]is exergy change flux of external heat source.

3. Results and discussion

3.1. Uncertainty

The temperature, pressure, mass flow, and power consumption were measured using the instruments specified in Section 2.1. The method proposed by Moffat [9] was used to calculate the maximum relative uncertainties of the experimental data (Equation 18). The relative uncertainty of COP arising with respect to the considered parameters are given by the following correlation [10],

$$\delta R = \left[\sum_{i=1}^{n}\left(\frac{\partial R}{\partial x_i}\delta x_i\right)^2\right]^{1/2} \tag{18}$$

$$\delta \mathrm{COP}_{\mathrm{heating}} = \left[\left(\frac{\Delta\dot{m}_{\mathrm{c}}}{\dot{m}_{\mathrm{c}}}\right)^2 + 2\left(\frac{\Delta T_{\mathrm{c}}}{T_{c,i} - T_{c,o}}\right)^2\right]^{1/2} \tag{19}$$

$$\delta \mathrm{COP}_{\mathrm{cooling}} = \left[\left(\frac{\Delta \dot{m}_{\mathrm{e}}}{\dot{m}_{\mathrm{e}}} \right)^2 + 2 \left(\frac{\Delta T_e}{T_{e,i} - T_{e,o}} \right)^2 \right]^{1/2} \quad (20)$$

Energy balances have been calculated based on the measured data, all of them were within the acceptable range. Thus, the measurements are reliable. Both water flow rate of condenser and evaporator were measured by ISOMAG-ML210 electromagnetic flowmeter with an accuracy of ±0.2 % and a range of 0 kg/s to 0.288 kg/s in the present study. The temperatures were measured by Type T thermocouples with an accuracy of ±0.5 ℃. The range of condenser side temperatures is from 29 ℃ to 62 ℃, thus, its maximum uncertainty was 1.6%; and for the evaporator side is from 15 ℃ to 36 ℃. Thus, its maximum uncertainty was 2.4 %. The maximum uncertainty in $\mathrm{COP}_{\mathrm{heating}}$ and $\mathrm{COP}_{\mathrm{cooling}}$ were 2.3 % and 3.4%, respectively.

Table 3 Tested results

No.	$T_{c,i}$	$T_{c,o}$	$T_{rc,i}$	$T_{rc,o}$	$T_{e,i}$	$T_{e,o}$	$T_{r,eo}$	P_c	P_e	W	Q_c	Q_e	$\mathrm{COP}_{\mathrm{heating}}$	$\mathrm{COP}_{\mathrm{cooling}}$	$\mathrm{COP}_{\mathrm{dual}}$	SH	Sub	Tesat	Tcsat	η_{ex}	$\eta_{II,dual}$
unit	℃	℃	℃	℃	℃	℃	℃	bar	bar	kW	kW	kW	-	-	-	K	K	℃	℃	%	%
1	30.4	48.9	70.6	44.5	22.7	17.3	18.0	13.1	4.4	1.13	3.89	3.16	3.43	2.79	6.23	6.0	5.3	12.0	49.8	14.8	20.1
2	30.4	56.9	77.0	46.3	22.2	16.8	17.6	15.1	4.4	1.13	4.04	3.15	3.57	2.78	6.35	5.7	9.0	11.9	55.4	19.4	25
3	30.3	57.0	77.4	44.6	22.1	16.7	17.8	15.1	4.4	1.13	4.02	3.14	3.55	2.78	6.32	6.2	10.9	11.6	55.6	19.3	25
4	30.0	60.0	80.3	44.9	22.1	16.8	17.9	16.0	4.4	1.16	4.01	3.11	3.45	2.67	6.12	6.2	12.9	11.8	57.9	20	25.3
5	38.5	52.7	74.2	48.4	23.6	18.1	18.9	14.3	4.5	1.15	4.10	3.19	3.57	2.78	6.35	6.1	5.0	12.8	53.4	21.2	25.6
6	29.9	56.3	75.9	46.8	22.1	16.7	17.8	14.9	4.4	1.13	3.97	3.11	3.51	2.75	6.26	6.0	8.2	11.9	55.0	18.6	24.2
7	30.1	59.6	77.5	49.3	22.0	17.0	15.1	15.9	4.5	1.16	3.95	3.00	3.4	2.58	5.98	2.8	8.4	12.3	57.7	19.6	24.6
8	35.9	46.7	67.3	40.8	22.1	17.0	14.9	12.8	4.4	1.13	4.28	3.41	3.78	3.01	6.79	3.0	7.9	11.9	48.7	18.1	24.3
9	39.9	55.2	73.1	46.3	22.0	17.0	13.8	15.3	4.5	1.18	4.09	3.11	3.47	2.63	6.1	1.2	9.8	12.6	56.1	22.8	27.9
10	40.3	55.4	74.4	48.8	22.7	17.7	14.9	15.3	4.6	1.15	4.05	3.09	3.53	2.69	6.22	1.9	7.2	13.0	56.0	23.2	27.9
11	38.5	54.2	73.0	49.8	23.6	19.3	16.6	14.8	4.7	1.16	4.20	3.26	3.6	2.8	6.4	2.5	5.0	14.1	54.8	22	25.9
12	39.4	53.6	70.3	50.5	21.9	16.9	13.3	14.6	4.5	1.15	3.81	2.90	3.32	2.52	5.84	1.1	3.7	12.2	54.2	20.9	25.9
13	34.1	57.4	73.3	51.9	22.0	17.1	13.8	15.5	4.5	1.2	3.80	2.85	3.18	2.38	5.56	1.1	4.7	12.7	56.6	19.3	23.7
14	40.3	50.2	67.9	48.7	22.7	17.5	13.8	13.8	4.5	1.15	3.90	3.05	3.4	2.66	6.06	1.4	3.2	12.4	51.9	20.1	24.9
15	40.0	50.0	72.1	47.6	21.9	16.6	16.4	13.7	4.4	1.13	3.94	3.07	3.48	2.71	6.19	4.8	3.8	11.6	51.4	20.4	26.1
16	43.6	53.4	75.7	50.5	22.2	17.1	16.7	14.8	4.4	1.16	3.89	2.98	3.34	2.56	5.91	4.6	4.3	12.1	54.8	22.8	27.7
17	40.1	55.0	76.2	50.4	22.6	17.8	17.2	15.0	4.5	1.16	3.98	3.05	3.42	2.62	6.04	4.5	4.9	12.6	55.3	22.3	26.9
18	48.5	58.7	80.7	57.0	27.0	21.6	21.4	16.9	5.0	1.24	4.10	3.12	3.29	2.5	5.8	5.6	3.2	15.9	60.3	26.1	27.2
19	44.7	54.6	77.0	52.3	23.1	18.0	17.7	15.3	4.6	1.2	3.92	2.99	3.28	2.5	5.77	4.7	3.7	13.0	56.0	23.3	27.3
20	34.2	58.3	78.3	50.4	22.0	16.9	16.6	15.6	4.4	1.16	3.89	2.96	3.35	2.54	5.89	4.5	6.5	12.1	56.9	20.7	25.6
21	34.2	60.0	79.8	51.3	22.1	17.1	16.7	16.2	4.5	1.2	3.88	2.94	3.24	2.45	5.7	4.5	7.0	12.2	58.3	20.9	25.4
22	48.1	58.5	80.2	56.7	26.9	21.5	21.3	16.8	5.0	1.2	4.11	3.13	3.44	2.62	6.06	5.3	3.4	16.0	60.1	26.9	28.2
23	45.2	60.6	81.2	56.9	27.1	21.7	21.6	17.2	5.1	1.21	4.15	3.14	3.42	2.59	6.01	5.4	4.0	16.2	60.9	26.3	27.4
24	44.0	58.3	79.5	54.1	22.6	17.7	17.4	16.2	4.6	1.2	3.84	2.88	3.21	2.41	5.62	4.5	4.4	13.0	58.5	24.2	28.1
25	42.9	59.3	80.4	55.6	35.4	22.6	24.6	16.7	5.3	1.23	4.42	3.43	3.6	2.79	6.39	7.0	4.0	17.6	59.6	24.9	22.5

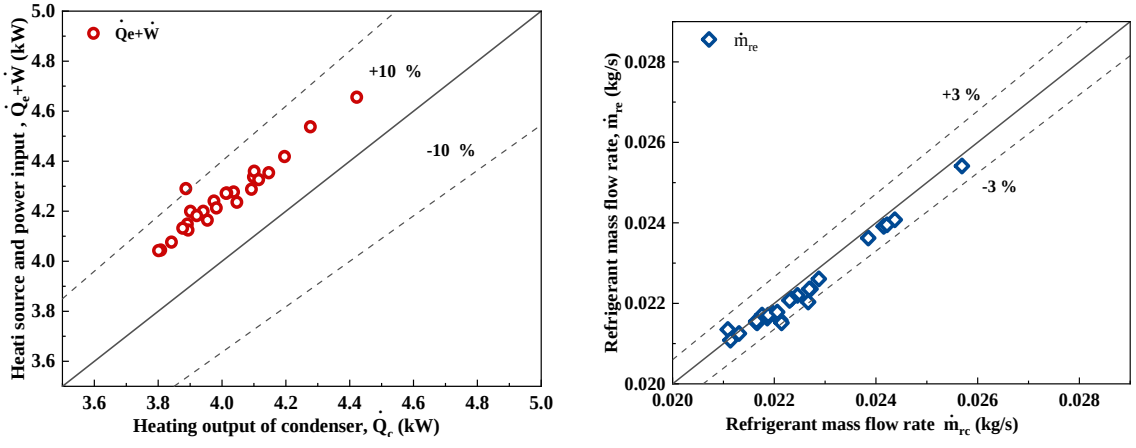

(a) (b)

Fig. 4. Uncertainty: a) Energy balance, b) Refrigerant flow rate calculation deviation.

3.2. Thermal performance

Under the proposed operation conditions of simultaneous cooling and heating the temperature of the hot water stream is increased by the heat release from the condenser while cooling down the temperature of cold water stream returned from the floor cooling system. The required temperature of the chilled/hot water differs depending on the demand, and thus sets the operation parameters of the heat pump and determines their efficiency.

Figure 5 summarizes the operation conditions of condenser and evaporator inlet and outlet temperature for the 25 test cases investigated in this study. The colour coding is according to the COP_{dual} reached under these operation conditions (See the colour bar at the bottom of Figure 5) . While Fig. 5a provides a complete overview of the tests, subfigures b-d display specific groups which will be discussed in the following paragraphs in a more detailed manner.

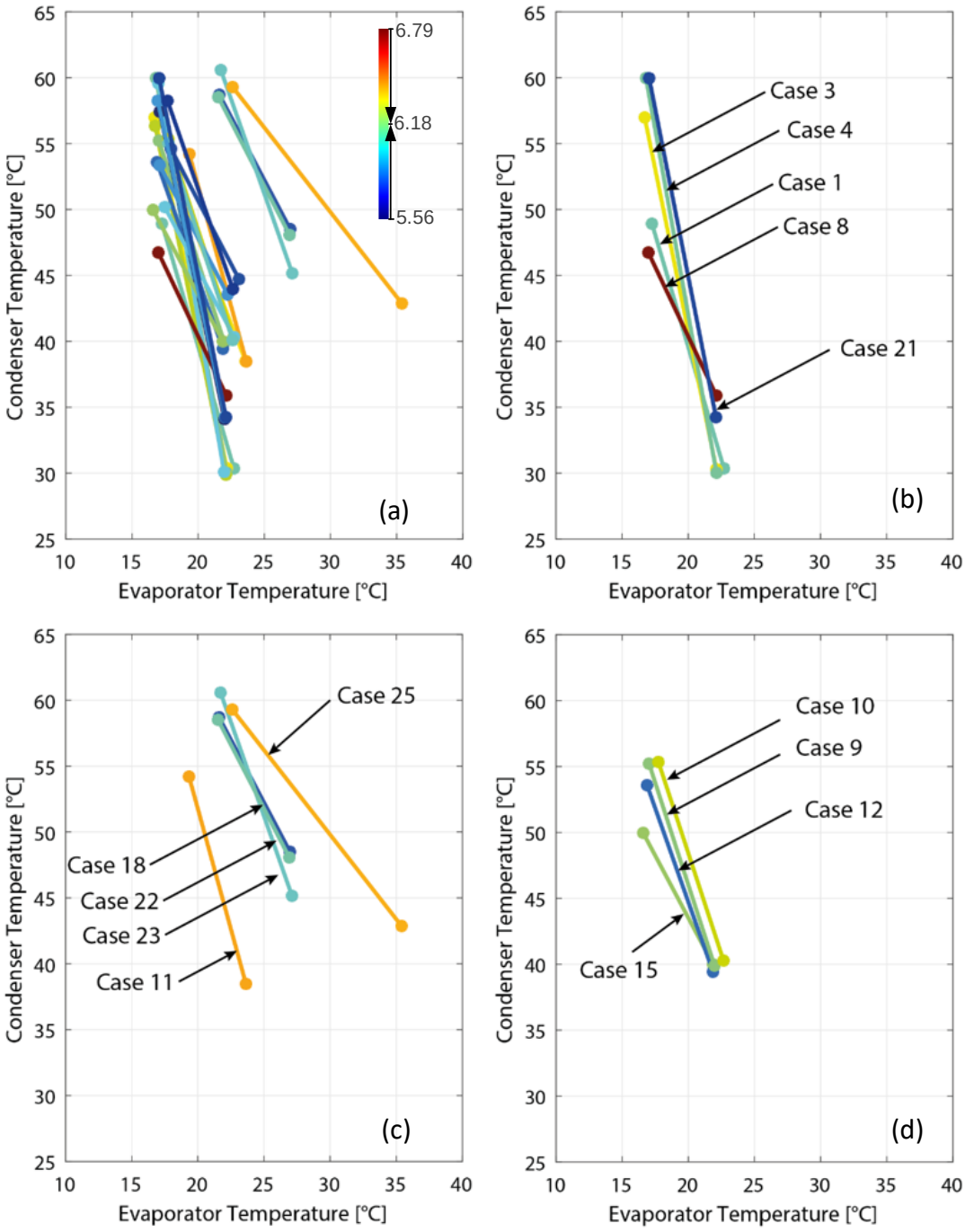

Fig. 5 Operation conditions of condenser and evaporator inlet and outlet temperature for the 25 test cases.

All cases displayed in Figure 5b have a low evaporator inlet temperature of 22 °C and an outlet temperature of 17 °C in common. They differ in the water temperature lift on the condenser side. Case 8 exhibits the highest COP_{dual} with a value of 6.79, which results from the low temperature lift from 35.9 °C to 46.7 °C in the condenser. The lowest COP_{dual} is measured for case 21, caused by the high temperature lift from 34.2 °C to 60.0°C. Increasing the temperature from 30 °C to 60 °C (case 4) results in a higher COP_{dual}. Both cases have a similar pressure level in the compressor. The difference in COP_{dual} is mainly attributed to the lower subcooling temperature reached in case 4 (12.9 K) compared to the subcooling temperature of 7.0 K in case 21. The same effect of the higher subcooling temperature is observed in a comparison of case 1 and case 3. Although the condenser outlet temperature is significantly higher for case 3 (57.0 °C) compared to case 1 (48.9 °C), the COP_{dual} is 0.1 points higher for case 3. Note the subcooling for case 3 is 10.9 K while this is only 5.3 K for case 1.

Figure 5c illustrates a second subset of cases. Note that case 18 and 22 have almost the identical inlet and outlet temperatures. Also all other measured quantities such as pressure and temperature levels are very similar. Nevertheless, the measured value of the COP_{dual} varies between 5.8 and 6.1, which is in the range of the measurement accuracy (5% difference), mainly caused by the given accuracy of the measured power consumption. Cases 11 and 25 both exhibit a high COP_{dual}. In case 25, the evaporator inlet temperature is high (35.4 °C) but also the evaporator outlet temperature is high (22.6 °C). The superheating in the evaporator is 7.0K at a saturation temperature of 17.6 °C. For case 11, the evaporator inlet temperature is 23.6 °C and the outlet temperature is only 19.3 °C. Due to the low temperatures, also the superheating in the evaporator is with 2.5K low. The high efficiency is caused by the low temperature at the condenser outlet of 54.2 °C. It reveals that a high temperature difference between condenser inlet and outlet temperature is beneficial for the COP due to the increased effect of subcooling and the higher subcooling temperature that can be achieved.

All cases shown in Figure 5d have same evaporator drop of around 5 °C. The highest $COP_{dual}$is measured for case 10, caused by the high evaporator inlet temperature of 22.7 °C. Compared with case 15, case 10 has a higher temperature lift from 40.3 °C to 55.4 °C, measured a lower superheating of 1.9 K and a higher subcooling of 7.2 K, which results in a higher COP_{dual} of 6.22. Case 12 exhibits the lowest COP_{dual} with a value of 5.84, which results from the lowest subcooling (3.7 K) among these compared four cases and the high temperature lift from 39.4 °C to 53.6 °C in the condenser. Case 15 has a lower temperature lift from 40.0 °C to 50.0 °C and a lower condenser outlet temperature (50.0 °C) than case 12, causing a high COP_{dual} of 6.19.

Figure 6 summarizes the exergy and second-law efficiency under operation conditions of condenser and evaporator inlet and outlet temperature for the 25 test cases investigated in the present study. The colour coding is according to the exergy efficiency (η_{ex}) /second-law efficiency ($\eta_{II,dual}$) reached under these operation conditions. Exergy efficiency is obtained by dividing the useful exergy gained from condenser by input exergy (Eq. (15)).

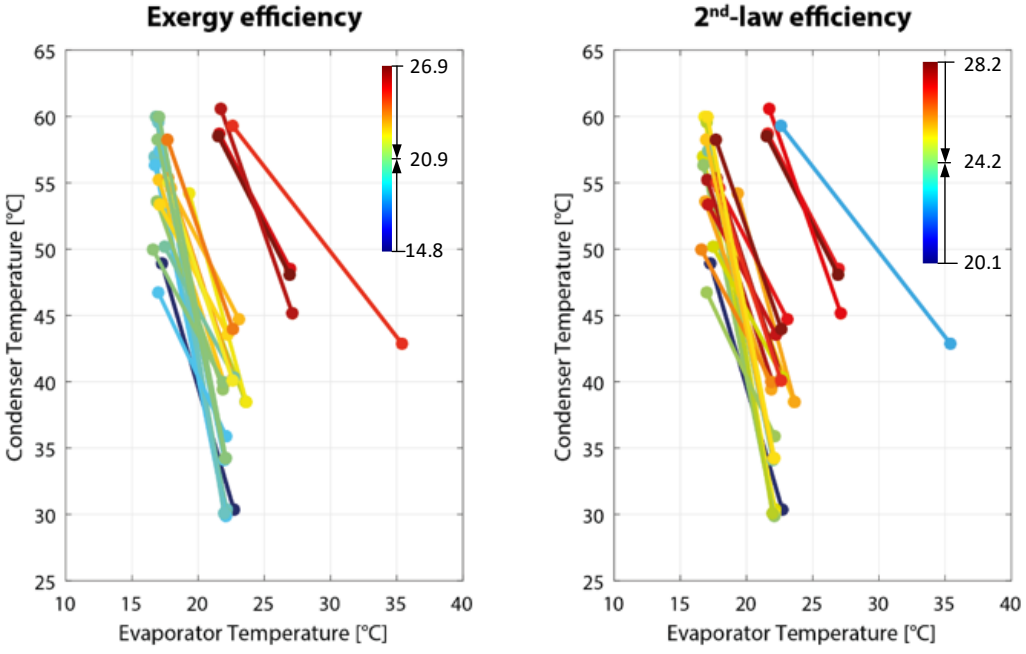

Fig. 6. Effect of condenser and evaporator inlet and outlet temperature on exergy efficiency and second-law efficiency.

Figure 6a shows an exergy efficiency distribution of the studied cases. Figure 6a shows that when the evaporator water inlet temperature ranged from 21.9 °C to 35.4 °C, the exergy efficiency varied from 14.8 to 26.9 %. The exergy efficiency increases with the increase of heat source temperature, which directly reflects the quality of the input energy. The decrease in the exergy efficiency is mainly attributed to the increase in compressor power with superheating degrees. Although Case 25 has a higher heat source temperature in the evaporator side, the temperature difference between inlet and outlet is also high. As the temperature difference increases, the irreversibility of the heat transfer process of evaporator increases, which results in a higher exergy loss corresponding a lower exergy efficiency than cases 18, 22 and 23.

The second-law efficiency of the simultaneous cooling and heating heat pump has been drawn in Fig. 6b based on the experimental results. Second-law efficiency achieved its maximum value at 28.2 % corresponding to a low temperature lift of condenser side and high temperature of DHW. Although the second law efficiency also shows the irreversibility of the system, different from exergy efficiency discussed above, $\eta_{II,dual}$ used in the present paper takes the useful output of $COP_{cooling}$ into consideration, which is numerically higher than exergy efficiency. Case 25 shows that the lower second-law efficiency ($\eta_{II,dual}$) is caused by a higher heat source temperature, with a very high ideal COP_{dual} such that $\eta_{II,dual}$ is significantly reduced to the corresponding 22.5 %.

3.3. Exergy efficiency

The performance of operation conditions with different heat sink temperatures have been studied experimentally. Mass flow rate of the comfort floor cooling water is fixed during testing these working conditions (m_e= 0.138 kg/s). Figure 9 shows five different working conditions with different DHW supply temperatures. The exergy and second law efficiency are highly influenced by the temperature of condenser side. Thus, an increment of the DHW temperature produces an increase of the energy quality and therefore, an increase of the efficiency. However, with the increase of DHW temperature, condensation temperature rises gradually, which make the system COP drop correspondingly.

Figure 9 also shows the exergy destruction ratio of each component in the studied simultaneous heat pump system. It can be found that the higher the temperature difference between inlet and outlet temperature of DHW, the lower the compressor exergy destruction ratio. The higher the temperature lift in the condenser side, the higher exergy destruction ratio of the condenser. The condenser side will be the potential component to improve the performance by decreasing the temperature lift when the evaporator side is fixed.

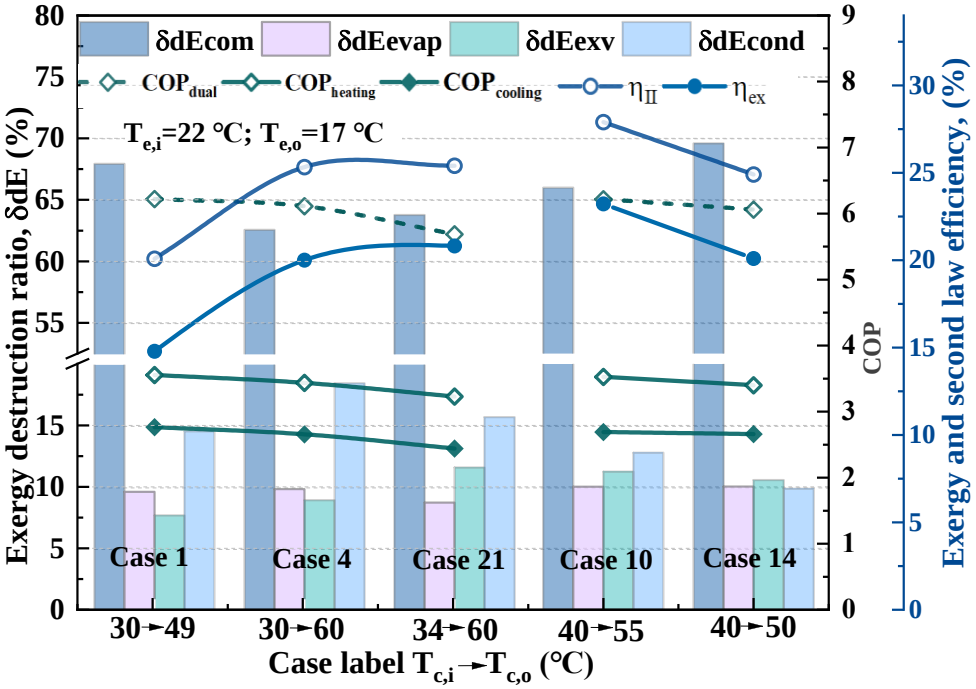

Fig.9. Effect of temperature difference on DHW side on heat pump system simultaneous performance.

4. Conclusions

A prototype of a water-source heat pump for simultaneous heating and comfort floor cooling was built and tested. Based on the experimental results discussed above, the main conclusions of the present study on steady state behavior of the proposed BHP can be drawn as follows,

- It can be found that the $COP_{heating}$ value varies from 3.0 to 3.4 in the studied conditions, and the $COP_{cooling}$ value ranged from 2.22 to 2.81. Test results showed that the cooling capacity ranged from 2.9 kW to 3.4 kW, heating capacity ranged from 3.8 kW to 4.4 kW.
- The lower domestic water temperature and higher temperature lift in the condenser can achieve a higher $COP_{heating}$ under the studied conditions with fixed cooling settings. A high temperature difference between condenser inlet and outlet temperature is beneficial for the COP_{dual} due to the increased effect of subcooling and the higher subcooling temperature that can be achieved.
- For each cooling load, there exists a corresponding heating capacity area, which can be used to regulate the system to operate at high efficiency. The highest dual-effect COP of the studied is 6.79. The second-law efficiency of the simultaneous DHW heating and floor cooling can reach 28.2 % within the studied range.
- The next step is to do the study with ratio of simultaneous DHW heating and cooling needs into consideration. System performance under non-synchronized DHW and cooling demands.

Acknowledgements

The authors gratefully acknowledge the financial support provided by Danfoss on the Comfort Cooling Project. The research also has received funding from the European Union's Horizon 2020 research and innovation program under the Marie Sklodowska-Curie grant agreement no. 713683 (COFUNDfellowsDTU, H. C. Ørsted Postdoc project HPMixPerform: Performance optimization of heat pumps using zeotropic mixtures as working fluid). The authors would also like to express our heartfelt gratitude to Jan Horne Hansen and Benny Edelsten for their help with the test rig.

Nomenclature

Symbols			
COP	Coefficient of Performance	P	Pressure (bar)
c_p	Specific heat capacity (J/(kg· K)	$\dot{Q}$	Energy capacity (kW)
DH	District heating	s	Entropy (kJ/kg·K)
$\dot{E}$	Exergy flow (W)	t	Temperature (℃)
$\dot{F}$	Volume flow rate of water (l/ h)	T	Temperature (K)
h	Specific enthalpy (kJ/kg)	$\dot{W}$	Compressor power (kW)
$\dot{m}$	Mass flow rate (kg/s)	y	Exergy destruction ratio
Subscripts			
comp	Compressor	L	Low
c	Condenser	o	Outlet
d	Exergy destruction	P	Production
e	Evaporator	r	Refrigerant
ex	Exergy	sub	Subcooling
ExV	Expansion valve	sup	Superheat
f	Forward	sat	Saturation state
F	Fuel	w	Water
H	High	0	Dead state
HS	Heat source	1,2,3,4	State point
i	Inlet	II	Second law
l	loss		
Greek Symbol			
Δ	Variation (-)	δ	Variation ratio (-)
η	Efficiency (%)		

References

[1] D.U. Shin, S.R. Ryu, K.W. Kim, Simultaneous heating and cooling system with thermal storage tanks considering energy efficiency and operation method of the system, Energy Build. 205 (2019). https://doi.org/10.1016/j.enbuild.2019.109518.

[2] F. Li, B. Sun, C. Zhang, L. Zhang, Operation optimization for combined cooling, heating, and power system with condensation heat recovery, Appl. Energy. 230 (2018) 305–316. https://doi.org/10.1016/j.apenergy.2018.08.101.

[3] X. Qin, Y. Zhang, D. Wang, J. Chen, System development and simulation investigation on a novel compression/ejection transcritical CO2 heat pump system for simultaneous cooling and heating, Energy Convers. Manag. 259 (2022) 115579. https://doi.org/10.1016/J.ENCONMAN.2022.115579.

[4] P. Byrne, R. Ghoubali, Exergy analysis of heat pumps for simultaneous heating and cooling, Appl. Therm. Eng. 149 (2019) 414–424. https://doi.org/10.1016/j.applthermaleng.2018.12.069.

[5] D.S. Ayou, R. Hargiyanto, A. Coronas, Ammonia-based compression heat pumps for simultaneous heating and cooling applications in milk pasteurization processes: Performance evaluation, Appl. Therm. Eng. 217 (2022) 119168. https://doi.org/10.1016/J.APPLTHERMALENG.2022.119168.

[6] D. Wu, B. Hu, R.Z. Wang, Performance simulation and exergy analysis of a hybrid source heat pump system with low GWP refrigerants, Renew. Energy. 116 (2018) 775–785. https://doi.org/10.1016/j.renene.2017.10.024.

[7] E.W. Lemmon, I.H. Bell, M.L. Huber, M.O. McLinden, NIST Standard Reference Database 23: Reference Fluid Thermodynamic and Transport Properties-REFPROP, Version 10.0, National Institute of Standards and Technology, (2018). https://doi.org/https://doi.org/10.18434/T4/1502528.

[8] A. Rijs, T. Mróz, Exergy Evaluation of a Heat Supply System with Vapor Compression Heat Pumps, Energies. 12 (2019) 1028. https://doi.org/10.3390/en12061028.

[9] R.J. Moffat, Describing the uncertainties in experimental results, Exp. Therm. Fluid Sci. 1 (1988) 3–17. https://doi.org/10.1016/0894-1777(88)90043-X.

[10] T. Zhu, T. Ommen, W. Meesenburg, J.E. Thorsen, B. Elmegaard, Steady state behavior of a booster heat pump for hot water supply in ultra-low temperature district heating network, Energy. 237 (2021) 121528. https://doi.org/10.1016/J.ENERGY.2021.121528.